Characterization of superconducting Ti transition edge sensors with different microbridge length

W. Zhang[1,2], J.Q. Zhong[1,2], W. Miao[1,2], Q.J. Yao[1,2], D. Liu[1,2], Z. Wang[1,2], S.C. Shi[1,2,*], T.J. Chen[3], L. H. Chang[3], M.J. Wang[3], D. Prele[4], F. Voisin[4], M. Piat[4] and F. Pajot[5]

[1]*Purple Mountain Observatory, CAS, China*
[2]*Key Lab of Radio Astronomy, CAS, China*
[3]*Institute of Astronomy and Astrophysics, Academia Sinica, Taipei*
[4]*Laboratoire AstroParticule et Cosmologie, Univ. Paris-7, France*
[5]*Institut d'Astrophysique Spatiale, CNRS - Univ. Paris-Sud, France*
*Contact: scshi@pmo.ac.cn, phone +86-25-8333 2204

Abstract—**We report on the performance of superconducting Ti transition edge sensors (TES) with different microbridge length varying from 1μm to 2.7μm. The TES devices are based on thin Ti film, evaporated on a high-resistivity silicon substrate. The current-voltage characteristics are measured at different bath temperatures using commercial SQUID amplifiers, from which the thermal conductance (G) is obtained. We also measure the current noise at different bias voltages. The obtained electrical noise equivalent power (NEP) from its calculated current responsivity and measured current noise is about $5\mathrm{x}10^{-17}$W/√Hz, which is low enough for ground-based terahertz superconducting imaging array (TeSIA), aiming at Dome A, Antarctica.**

I. INTRODUCTION

THE far-infrared/sub-millimeter band contains a wealth of information about the cold universe. Observations of gas and dust can probe the earliest stages in the formation of galaxies, stars and planets. For example, SCUBA-2, containing 10,000 superconducting transition-edge sensors (TESes), has been mounted on the James Clerk Maxwell Telescope (JCMT) and continuously carries out astronomical observations [1]. POLARBEAR [2] and ACTPol [3] are devoted to directly measure the gravitational lensing in the polarization of the Cosmic Microwave Background. In China, Purple Mountain Observatory is leading the efforts on a 5-m THz telescope (DATE5) [4] to be constructed at Dome A, the highest point on the Antarctic plateau at an elevation of 4100 m. The atmospheric transmission above Dome A is 80% at 661 GHz during the Austral winter, corresponding to a perceptible water vapour column of 0.1 mm. Dome A has been confirmed to be an ideal site on earth for terahertz astronomy with a Fourier transform spectrometer [5]. The first generation instrument of DATE5 is a highly sensitive heterodyne receiver at 200 μm and 350 μm. Its next generation will be a direct detector array with background limited sensitivity, i.e. noise equivalent power (NEP) ~10^{-16} W/√Hz. We are currently developing a terahertz superconducting imaging array (TeSIA) for DATE5 at 350 μm, and TESes are one potential detector candidate. Superconducting Ti bolometric detectors with a critical temperature of ~500mK are of particular interest because of simple structure and high sensitivity [6]. Here we present the details of the detector fabrication and electrical characterization.

II. SUPERCONDUCTING TESES AND MEASUREMENT SETUP

Our superconducting TES devices are based on a Ti film, which is evaporated on a 400μm high-resistivity Si substrate. The micro-bridge is patterned by optical lithography. RF cleaning is used to remove the TiOx on the surface of Ti film before deposition of the 150 nm thick Nb contacts. It should be noted that we don't back etch the support Si substrate under the Ti microbridge, therefore the heat can be relaxed by electron diffusion and electron-phonon interaction. Fig.1 shows the Ti TES devices with 1μm (a) and 2.7μm (b) microbridge length, respectively. The contact pads with large area are designed to reduce the contact resistance. As exhibited in Fig. 1c, Ti Film on Si substrate is about 38 nm thick, and there is a natively oxidized layer on the surface of the Si substrate [7]. Within the microbrige region, there is a white layer with a thickness of 32 nm between Si substrate and Ti film, which might be formed during the etch process of Nb. The Ti TES device parameters are listed in Table 1. R_N is the normal resistance of Ti TES devices.

Table1 Parameters of Ti TES devices

Device	Substrate	LengthxWidth (μm x μm)	Thickness (nn)	R_N (Ω)
1	Si	1.2x1.0	37.5	18
2	Si	2.7x1.4	37.5	54

The Ti TES devices are tested using an Oxford Triton 400 dilution cooler [8] that is able to cool the device down to 20 mK. The Ti TES devices are glued to the copper holder with VGE-7031 vanish. The constant voltage is realized by using a 0.68 Ω resistor (R_{SH}) in parallel with the Ti TES device, which is then connected to the input coil of a Magnicon single-stage SQUID [9] via twisted superconducting wires. The input inductance of the SQUID is 150 nH, and its current noise contribution is about 1pA/Hz$^{0.5}$. The TES current is read out by the SQUID with a closed flux locked loop.

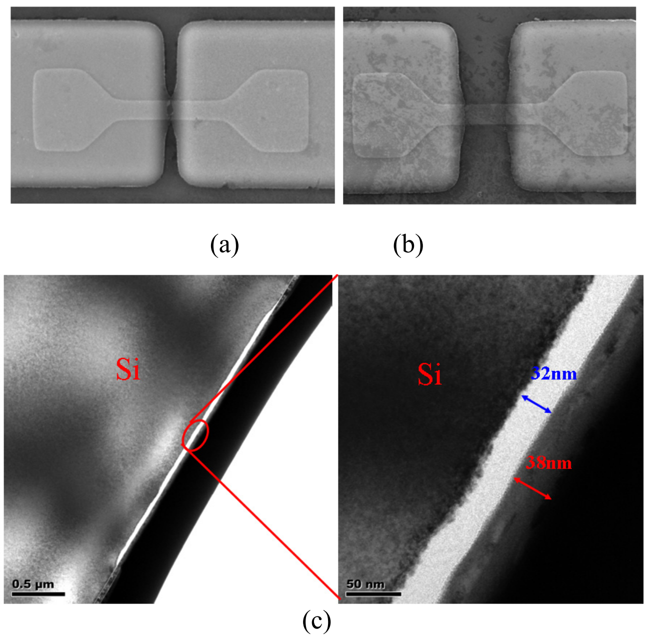

Fig.1 SEM photos of superconducting Ti transition edge sensors with microbridge dimension of 1µm x 1µm (a) and 2.7 µm x 1.4 µm (b). (c) TEM image of Ti TES device with 2.7µm long microbridge length, which shows the Si substrate and 38 nm thick Ti microbridge. There is a 32 nm thick white layer between Si substrate and Ti film in the microbridge region.

III. CURRENT-VOLTAGE CHARACTERISTICS

We have measured the current-voltage characteristics of the Ti TES device with 2.7µm long microbridge while changing the bath temperature from 20 mK to 500 mK. The TES current (I_{TES}) can be directly calculated from the output voltage with the SQUID amplifier gain. R_N and parasitic resistance (R_{PAR}) are determined from its normal and superconducting branches from the measured I-V curves, respectively. Then the TES voltage (V_{TES}) is calculated using the Thevenin equivalent circuit model [10] and plotted in Fig. 2. As shown in Fig.3a, the DC power in the transition increases with bias voltage due to the fact that the underneath Si substrate is not etched. We choose the data points of the Ti TES device at 20 Ω and 40 Ω, corresponding to 40%R_N and 80%R_N, respectively, and plot the power level as a function of bath temperature (see Fig.3b).

The heat flow equation for the Ti TES device can be written as [10]:

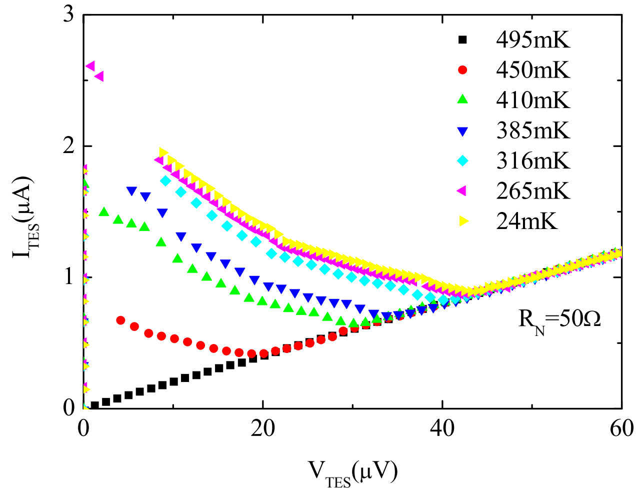

Fig.2 Current-voltage curves of the NbSi TES device at different bath temperatures. V_{TES} and I_{TES} are the voltage and current of the NbSi TES.

$$P_{DC} = K(T_c^n - T_{bath}^n)\,, \qquad (1)$$

where P_{DC} is the DC bias power applied to the TES device, K is a constant that depends on the geometry and material properties of the supporting structure, and n is the thermal-conductance exponent, which depends on the dominant thermal transport mechanism. We can fit Eq. (1) to the measured data to find K, n and T_c. For this device the best fits are obtained using n=5 and T_c=470 mK, which is consistent with that found in [11]. Thermal conductance (G) between the TES device and the substrate can be easily obtained as $G=nKT_c^{n-1}$=319 pW/K and 400 pW/K for 40%R_N and 80%R_N, respectively.

The fundamental phonon noise determined NEP can be calculated from the obtained thermal conductance as $NEP_{phonon}= (2k_BT^2G)^{0.5}$ =4.4~4.9x10^{-17} W/√Hz, where k_B is the Boltzmann constant.

IV. CURRENT NOISE

Fig. 4a shows the measured current noise spectra at different bias voltages in the transition at the bath temperature of 410 mK. The spikes in the spectra are due to the electromagnetic interference from the 50-Hz power line, which can be further shielded. The current noise spectra are relative high at lower frequencies due to the mechanical vibration and temperature fluctuation of the pulse-tube refrigerator. Therefore we choose the current noise at 10 kHz and plot it as a function of bias voltage in Fig. 4b. At large bias voltage, the current noise is reduced at frequencies beyond 1 kHz since Ti TES device enters normal state. However it is still higher than the current noise contribution of SQUID, indicating that there are some excess noises, which is still not unclear. Dividing the measured current noise by the current responsivity (S_I) yields the electrical NEP at each operating point. The current responsivity at low frequency can be simply written as $S_I=1/I_{TES}(R_{TES}-R_L)$, where R_{TES} is the DC resistance of the TES device, and R_L is the load resistance in the bias circuit ($R_{SH}+R_{PAR}$) [10]. The average electrical NEP at

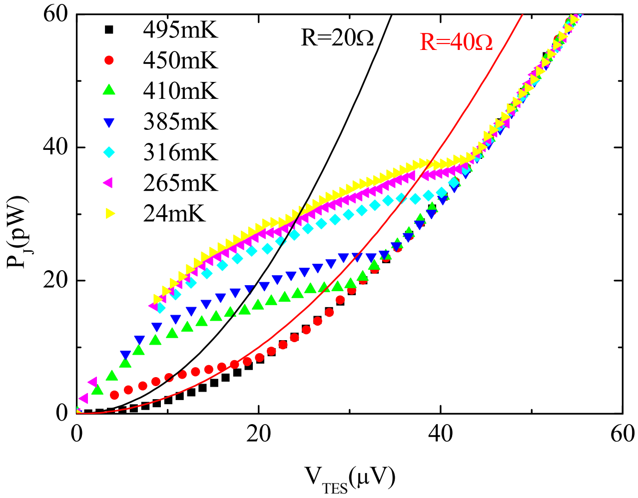

(a)

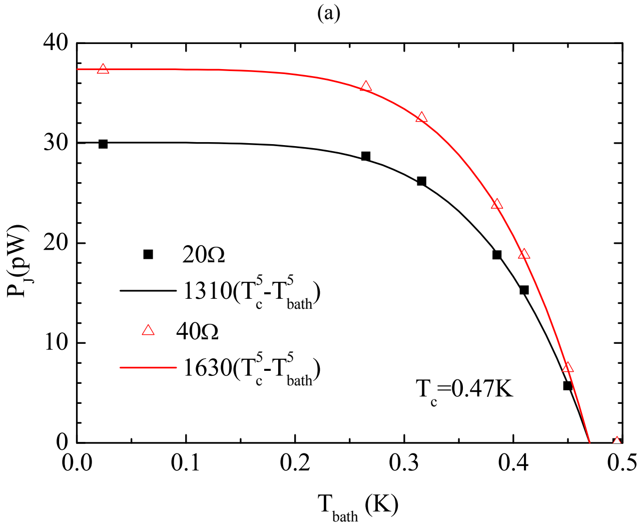

(b)

Fig. 3 (a) DC power of the Ti TES device as a function of bias voltage. The black and red lines show the DC power of 20Ω and 40Ω resistors at constant voltage. (b) Power level of the Ti TES device in the transition as a function of bath temperature.

all bias points within the transition is ~$5\text{x}10^{-17}$ W/√Hz, which is close to NEP_{phonon}.

V. Conclusions

We are measuring the other Ti TES device with shorter microbridge length, and its NEP should be smaller since the NEP scales as the square root of microbridge volume [12]. Furthermore we are going to measure the complex impedance, and the response time will be obtained.

In conclusion, we have tested the electrical performance of a superconducting Ti TES for TeSIA. The thermal conductance extracted from the measured I-V characteristics at different bath temperatures is 300~400 pW/K, which corresponds to a phonon noise dominated NEP of 4.4~$4.9\text{x}10^{-17}$ W/√Hz. Our noise measurement shows an electrical NEP of about $5\text{x}10^{-17}$ W/√Hz, which is close to the phonon noise dominated NEP. A large TES array with background limited sensitivity is suitable for ground-based application at Dome A, Antarctica.

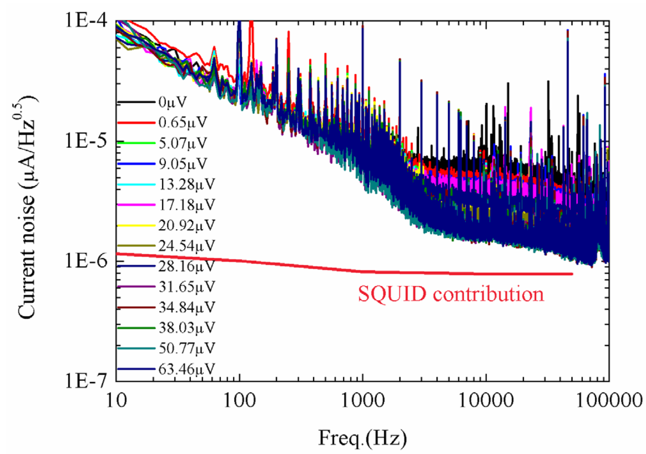

(a)

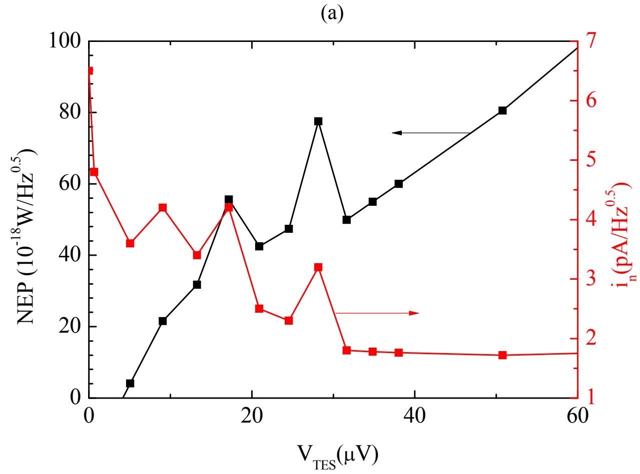

(b)

Fig. 4 (a) Current noise spectrum of the Ti TES device at different bias voltages. (b) Current noise at 10 kHz and corresponding noise equivalent power of the Ti TES device as a function of bias voltage.

Acknowledgment

The authors would like to thank K. Zhang and F. Wu for their technical support.

References

[1] W. S. Holland, D. Bintley, E. L. Chapin, A. Chrysostomou, G. R. Davis, et al, “SCUBA-2: the 10000 pixel bolometer camera on the James Clerk Maxwell Telescope,” *Mon. Not. R. Astron. Soc.* 430, 2513, 2013.

[2] K. Arnold, P.A.R. Ade, A.E. Anthony, F. Aubin, D. Boettger, et al, “The POLARBEAR CMB polarization experiment,” *Proc. of SPIE*, vol.7741, 77411E, 2010.

[3] M.D. Niemack, P.A.R. Ade, J. Aguirre, F. Barrientos, J.A. Beall, et al, “ACTPol: A polarization-sensitive receiver for the Atacama Cosmology Telescope,” *Proc. of SPIE*, vol.7741, 77411S, 2010.

[4] J. Yang, Y.X. Zuo, Z. Lou, J.Q. Cheng, Q.Z. Zhang, et al, “Conceptual design studies of the 5m terahertz antenna for Dome A, Antarctica,” Research in Astron. Astrophys. vol.13 (12), pp.1493-1508, 2013.

[5] S.C. Shi, M. Ashley, Z. H. Shang, Z. W. Hu, S. Paine, et al, “A Fourier transform spectrometer for atmospheric measurements at Dome A,” IAU 2012, Aug.20-31, 2012.

[6] B.S. Karasik, A.V. Sergeev, and D.E. Probe, “Nanobolometers for THz photon detection,” IEEE Trans. Terahertz Sci. technol.1(1), pp.97-111, 2011.

[7] W. Zhang, W. Miao, J.Q. Zhong, S.C. Shi, D.J. Hayton, N. Vercruyssen, J.R. Gao, and G.N. Goltsman, “Temperature dependence of the receiver noise temperature and IF bandwidth of superconducting

hot electron bolometer mixers," Supercond. Sci. Technol.27, 085013, 2014.

[8] Triton TM 200/400, Cryofree dilution refrigerator, Issue 3.0, Oxford instruments, 2012.

[9] High performance dc SQUID electronics, XXF-1 manual, v3.3.11, Magnicon physical research and instrumentation, 2013.

[10] K.D. Irwin and G.C. Hilton, Transition-edge sensors, in Cryogenic Particle Detection. Topics in Applied Physics, vol.99 (Springer, Berlin, 2005).

[11] J. Wei, D. Olaya, B.S. Karasik, S.V. Pereverzev, A.V. Sergeev, and M.E. Gershenson, " Ulatrsensitive hot-electron nanobolometers for terahertz astrophysics," Nature nanotechnology, 3, pp.496-500, 2008.

[12] B.S. Karasik, S.V. Pereverzev, D. Olaya, J.Wei, M.E. Gershenson, and A. V. Sergeev, "Nooise measurements in hot electron Ti nanobolometers," IEEE Trans. Appl. Supercond. 19 (3), pp. 532-535, 2009.